ADVANCES IN ATMOSPHERIC SCIENCES, VOL. 29, NO. 3, 2012, 519–528

Simulations of the Motion of Tropical Cyclone-like Vortices in the Presence of Synoptic and Mesoscale Circulations

LUO Zhexian[1] (罗哲贤) and PING Fan*[2] (平 凡)

[1]*Key Laboratory of Meteorological Disaster of Ministry of Education, Nanjing University of Information Science and Technology, Nanjing* 210044

[2]*Laboratory of Cloud-Precipitation Physics and Severe Storms, Institute of Atmospheric Physics, Chinese Academy of Science, Beijing* 100029

(Received 13 October 2011; revised 23 December 2011)

ABSTRACT

Initial mesoscale vortex effects on the tropical cyclone (TC) motion in a system where three components coexist (i.e., an environmental vortex (EV), a TC, and mesoscale vortices) were examined using a barotropic vorticity equation model with initial fields where mesoscale vortices were generated stochastically. Results of these simulations indicate that the deflection of the TC track derived from the initial mesoscale vortices was clearly smaller than that from the beta effect in 60% of the cases. However, they may have a more significant impact on the TC track under the following circumstances. First, the interaction between an adjacent mesoscale vortex and the TC causes the emergence of a complicated structure with two centers in the TC inner region. This configuration may last for 8 h, and the two centers undergo a cyclonic rotation to make the change in direction of the TC motion. Second, two mesoscale vortices located in the EV circulation may merge, and the merged vortex shifts into the EV inner region, intensifying both the EV and steering flow for the TC, increasing speed of the TC.

Key words: cyclone-like vortices, synoptic and mesoscale circulations

Citation: Luo, Z. X., and F. Ping, 2012: Simulations of the motion of tropical cyclone-like vortices in the presence of synoptic and mesoscale circulations. *Adv. Atmos. Sci.*, **29**(3), 519–528, doi: 10.1007/s00376-011-1199-9.

1. Introduction

Tropical cyclone (TC) motion may arise from environmental currents, the beta effect, or asymmetric convection (Elsberry, 1995). Many of the characteristics of TC motion may be explained as a small vortex that is being advected by a large-scale environmental flow (steering concept, or cork-in-a-stream concept; Chan and Gray, 1982; DeMaria, 1985; Dong and Neumann, 1986; Velden and Leslie, 1991; Wu and Kurihara, 1996; Wang et al., 2006; Wu et al., 2006). The beta effect can be better understood using theoretical and numerical studies (Chan and Williams, 1987; Fiorino and Elsberry, 1989; Tian and Luo, 1994; Wu and Wang, 2000; Chan et al., 2002; Yu et al., 2006). In this study, asymmetric convection effects on TC motion were analyzed extensively. Willoughby (1992) indicated that a mesoscale convective system near a TC center may cause track meanders on shorter time scales of 4–12 h. Chen and Luo (2006) showed that when a small vortex appears in the northeast quadrant of TC circulation, the TC turns leftward with prominent oscillation. Luo and Liu (2006) demonstrated the complexity of a major vortex motion in a system where four subsystems with different scales coexisted (a subtropical high ridge, a major vortex, meso- and small-scale vortices), and three kinds of major vortex tracks were observed.

As indicated by Elsberry (2007), the problem of TC track prediction is more difficult than the simple description above because each of these components varies in time and they interact in a nonlinear man-

*Corresponding author: PING Fan, pingf@mail.iap.ac.cn

ner. The key point is that TC motion is a multi-scale, nonlinear interaction problem.

In this study, we explored the problem of TC track deflection in a multi-scale nonlinear system based on large sample analyses. The brief description of the methodology is given in next section. Preliminary results on mesoscale vortex effects on a TC track in a three-component system [an environmental vortex (EV), the TC, and mesoscale vortices] are presented in section 3. In section 4 the possible mechanisms responsible for impacts of mesoscale vortices on the tracks of TCs are discussed. A summary is presented in section 5.

2. Methodology

2.1 *Model*

Vortex dynamics in two dimensions can be described by the following equation governing the evolution of the relative vorticity:

$$\frac{\partial}{\partial t}\nabla^2\psi + J(\psi, \nabla^2\psi) + \beta\frac{\partial\psi}{\partial x} = -\nu\nabla^4\psi \qquad (1)$$

where ψ is geostrophic stream function, $\xi = \nabla^2\psi$ is relative vorticity, J is Jacobian operator, $\beta = 2\Omega\sin\varphi$ with Ω being the angel velocity of the Earth's rotation and φ is the latitude; ν is the hyper-viscosity coefficient, which compresses the dissipation range into a smaller range of scales (Basdevant et al., 1981), ν=1.0×10^{-7} m^4 s^{-1} (Ishioka et al., 2006), and ∇^2 the Laplacian in x and y.

The computational domain is a square of 1200 km×1200 km with a resolution of $\triangle x = \triangle y$=3 km and total of 401×401 grid points. The time step is taken as $\triangle t$=30 s for integration. The time-filter central difference scheme (Asselin, 1972) is employed at every time step to suppress nonlinear instability.

2.2 *Boundary and initial conditions*

At the eastern and western borders of the domain, periodic conditions were assumed, while $\dfrac{\partial\psi}{\partial t} = 0$ is set at the north and south borders:

At t=0, set

$$\xi(x, y, 0) = \xi_{\rm d}(x, y, 0) + \xi_{\rm s}(x, y, 0)\ , \qquad (2)$$

where $\xi_{\rm d}(x, y, 0)$ denotes a deterministic vorticity field, which consists of two larger scale vortices:

$$\begin{aligned}&\xi_{\rm d}(x, y, 0) = \\ &\xi_{\rm d0}\sin\left(\frac{x - x_{11}}{x_{12} - x_{11}}\pi\right) \times \sin\left(\frac{y - y_{11}}{y_{12} - y_{11}}\pi\right) + \\ &\xi_{\rm d0}\sin\left(\frac{x - x_{21}}{x_{22} - x_{21}}\pi\right) \times \sin\left(\frac{y - y_{21}}{y_{22} - y_{21}}\pi\right)\ , \end{aligned} \qquad (3)$$

where $\xi_{\rm d0}$=4.0×10^{-4} s^{-1} and the radius of the two vortices are 100 km. Let $(x_0, y_0) = (600, 600)$ km, (x_0, y_0) denotes the computational domain center; $(x_{11}, x_{21}) = (261, 516)$ km, (x_{21}, x_{22})=$(684, 939)$ km, $(y_{11}, y_{21}) = (450, 750)$ km, $(y_{21}, y_{22}) = (450, 750)$ km; $\xi_{\rm s}(x, y, 0)$ denotes a mesoscale vorticity field, which is determined stochastically. The starting conditions consist of uniform vorticity vortices with an equal number having $\xi_{s0} = 3.0 \times 10^{-4}$ s^{-1} and with an equal radius of 27 km (Reinaud et al., 2003). The starting conditions consist of uniform vorticity vortices. With an equal number having $\xi_{s0} = 3.0 \times 10^{-4}$ s^{-1} and with an equal radius being 27 km (Reinaud et al., 2003). The total circulation for each of the initial mesoscale vortices is 2.75×10^6 m^2 s^{-1}. Gentry et al. (1968) reported the low-level convergence field for a large convective asymmetry derived from aircraft observations of Hurricane Gladys. Atlantic Hurricane Gladys lasted for the period of 13–21 October 1968. Enagonio and Montgomery (2001) estimated the total circulation for the asymmetry to be approximately 1.9×10^6 m^2 s^{-1}, which is similar to the total circulation used in this work. The mesoscale vortices are randomly positioned in space with care to ensure that they do not overlap. When overlap of the initial stochastic vortices occurs, the vorticity in the overlapped area increases, resulting in the maximum initial stochastic vorticity value becoming too large in the area. In this study, 62 initial stochastic vorticity fields were generated, named SF$_1$, SF$_2$, …, SF$_{62}$, respectively. The number of stochastic vorticity fields was chosen somewhat artificially, but the 62 samples provided enough data for our study.

2.3 *Experimental design*

Two categories of experiments were performed: category A and category B. In category A, the initial stochastic vorticity field was omitted. EXA$_1$ further omitted the beta term, while EXA$_2$ included it. Category B included the initial stochastic vorticity fields. Initial stochastic vorticity fields SF$_1$, SF$_2$,…, SF$_{62}$, were introduced into EXB$_i$($i = 1, 2, \ldots, 62$), respectively. As indicated by Chan and Williams (1987), the streamfunction and relative vorticity are concentric initially for a symmetric vortex on a beta-plane with no mean flow in a non-divergent barotropic model. Only the beta term contributes to the vorticity tendency, inducing the production of an asymmetry in the vorticity field. Because of the asymmetry, the streamfunction and relative vorticity isolines are no longer concentric. The nonlinear advection processes are also included. The vortex propagates northwestward due to both the beta term and the nonlinear advection. The results of the track deflection from the experiments including beta term was compared with those

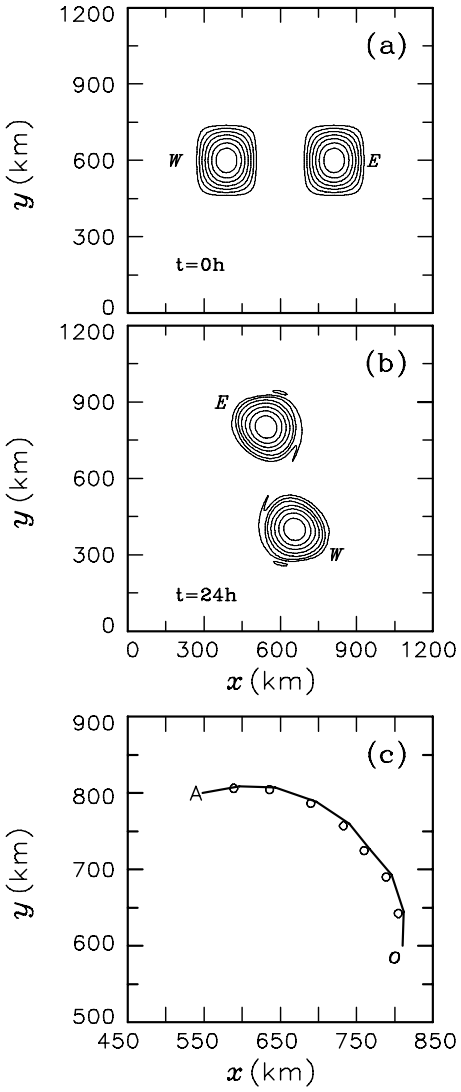

Fig. 1. Vorticity (contour interval 0.5×10^{-4} s^{-1}), at (a) t=0 and (b) 24 h, and the track of the TC(c) for EXA$_1$ without the beta effect or any initial mesoscale vortices. Circles indicate positions each 3 h.

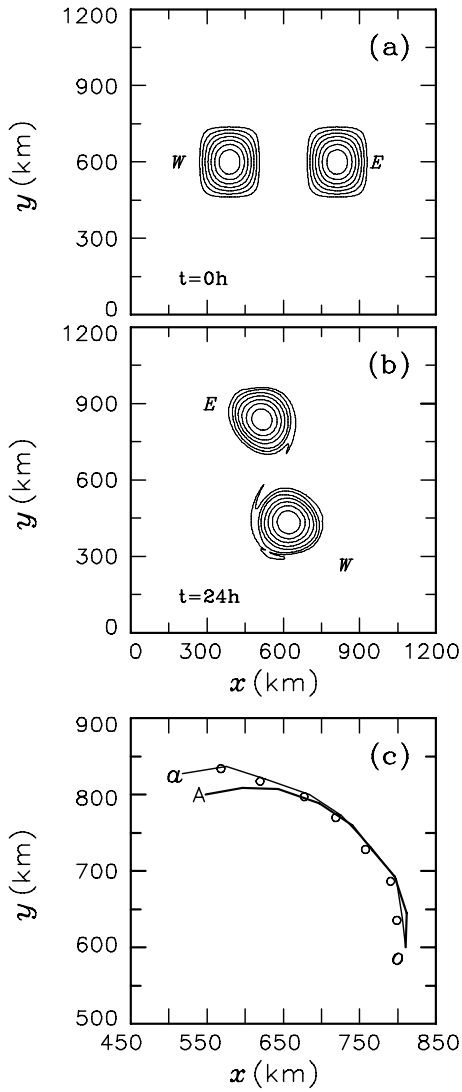

Fig. 2. As in Fig. 1 except for EXA$_2$ with the beta effect, track OA for EXA$_1$, and track Oa for EXA$_2$.

derived from the initial mesoscale vortices.

3. Preliminary results

3.1 *The track deflection caused by the beta effect*

The EXA$_1$ without both the beta effect and any initial stochastic vorticity fields was performed. In the initial vorticity field of this case there are two equal size cyclonic vortices ***W*** and ***E*** that are prescribed by Eq. (3) with a suitably small separation distance of 420 km (Fig. 1a). As indicated by Elsberry (2007), the environmental flow depends on the strength and positions of the monsoon trough and subtropical anticyclone, and on adjacent synoptic-scale circulations (trough, ridges, and perhaps another TC). Here, vortex ***W*** in Fig. 1a was chosen as an environmental vortex (EV), and vortex ***E*** is named as a TC. The EV and TC have a cyclonic rotation (Fig. 1b). In the steering of the outer tangential wind field of the EV, the TC moved northwestward with an average translation speed of ∼3.5 m s^{-1} during 0–24 h (Fig. 1c).

The EXA$_2$ with the beta effect and without any initial stochastic vorticity fields were performed. The vorticity fields at t=0 and 24 h are shown in Figs. 2a and b. Comparison of the TC tracks between the EXA$_1$ (OA in Figs. 1c and 2c) and the EXA$_2$ (Oa in Fig. 2c) indicates that a track deflection induced by the beta effect occurred. The value of the deflection was 40 km at t=24 h.

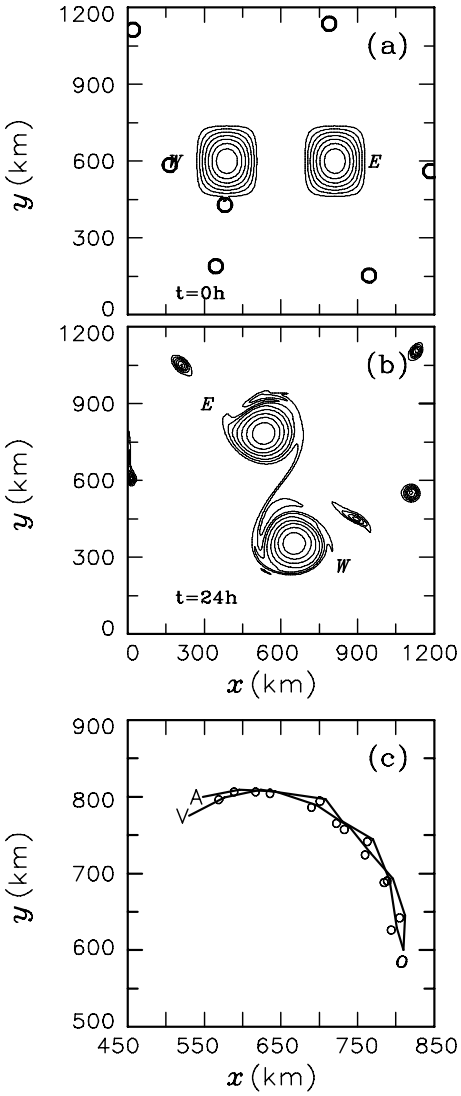

Fig. 3. As in Fig. 1 except for EXB_1 with the initial stochastic vorticity field SF_1, track OA for EXA_1, and track OV for EXB_1.

3.2 *The track deflection caused by the initial stochastic vorticity field in the case study*

The EXB_1 with the initial stochastic vorticity field SF_1 and without the beta effect was conducted. The vorticity distribution at t=0 and 24 h in the EXB_1 case is shown in Fig. 3. The deflection of the TC track at t=24 h was ~20 km, which was smaller than that deduced from the beta effect (Fig. 3c).

3.3 *The track deflection caused by the initial stochastic vorticity field: Statistics*

In this study, 62 simulations with various initial stochastic vorticity fields, SF_1, SF_2,..., SF_{62}, were conducted. Figure 4 indicates that many scattered points exist from the 62 simulations; they denote the TC center positions in the cases at t=24 h, respectively. As shown in Fig. 4, 37 scattered points were located inside the big circle. This means that the track deflections in 37 cases were smaller than those deduced from the beta effect. Other points outside the big circle represent the cases of larger track deflection.

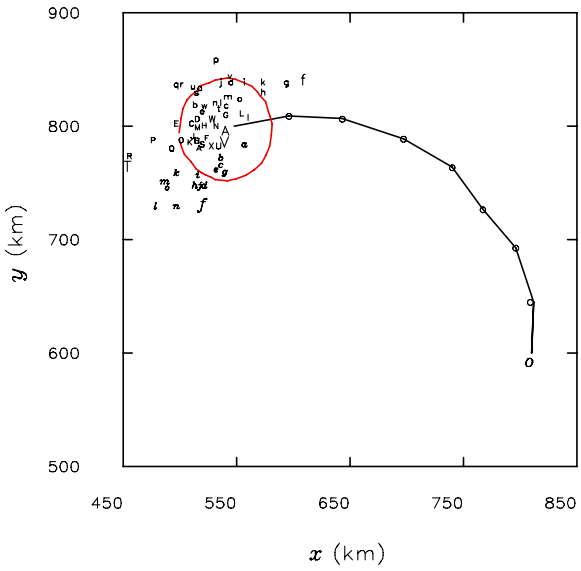

Fig. 4. Positions of the center of the TC derived from 62 simulations with various initial stochastic vorticity fields in EXB_i (i=1, 2, ... 62) at t=24 h, track OA for EXA_1, the big circle denotes the radius of deflection deduced from the beta effect.

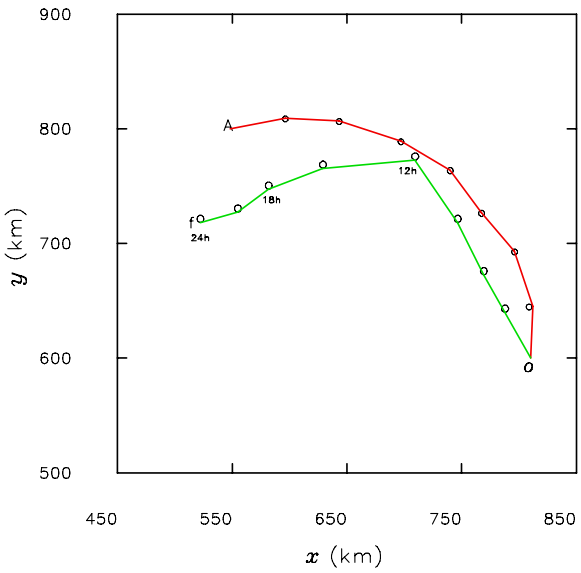

Fig. 5. Track of the center of the TC for EXA_1 (OA), and for EXB_2 (Of), circles denote TC center positions (3-h intervals).

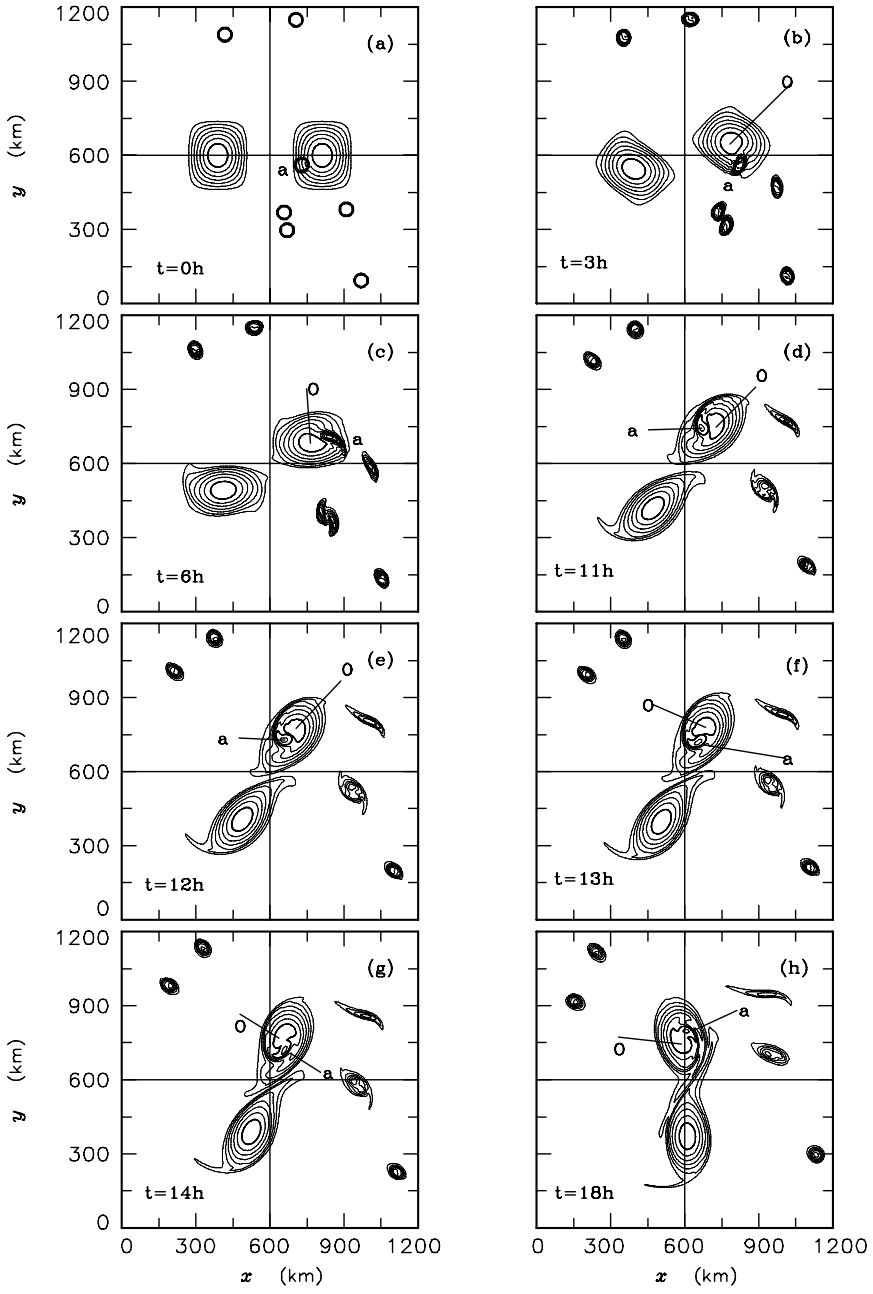

Fig. 6. Vorticity (contour interval 0.5×10^{-4} s^{-1}). At (a) t=0, (b) 3 h, (c) 6 h, (d) 11 h, (e) 12 h, (f) 13 h, (g) 14 h, and (h) 18 h for EXB_2.

3.4 *Possible mechanisms on the initial stochastic vorticity field effects on TC motion*

Here we wish to explore the possible mechanisms to explain why the initial stochastic vorticity field can affect the TC motion. As indicated by Elsberry (2007), the key point is that the TC motion is a multi-scale, nonlinear interaction problem. The TC motion should be viewed as a macroscopic behavior of a multi-scale, complex system in which the planetary vorticity, environmental currents, the TC, and the mesoscale vortices are involved. The essential point of view in Feynman's lecture (Feynman, 1961) was that the microscopic change of things at small scales could control the macroscopic characteristics at large scales. According to this point of view, once stochastically distributed mesoscale vortices are added into a deterministic initial field of a numerical model describing the TC motion, the possibility of unusual changes in direction and/or speed of TC motion is also simultane-

ously introduced. Based on this theory, we propose a hypothesis as follows. TC motion is governed by a multi-scale, nonlinear, complex system; the interaction among these scale components always exists according to two types of interaction: direct interaction and indirect influence. In the former, adjacent mesoscale vortices directly modify the structure of the TC. In the latter, they indirectly change the intensity of the environmental vortex as well as the steering currents. The both can eventually result in different macroscopic behavior (TC tracks).

3.4.1 *Direct interaction*

The simulations in EXB_2 and EXA_1 indicate that a significant track deflection occurred near t=12 h in EXB_2 (Fig. 5). Figure 6 depicts an evolution sequence of vorticity distribution in EXB_2. At t=0 h, a mesoscale vortex a was located the southwest to the TC center (Fig. 6a). During 0–6 h, vortex a had a cyclonic rotation around the TC center and suffered a distortion due to the tangential wind shear of the TC. The elongation of vortex a along the streamlines must be accompanied by contraction in the cross-stream direction to conserve absolute vorticity (Figs. 6a–c). Afterward there was a process similar to the self-organization of vorticity on scales of 40–50 km in the TC circulation, resulting in the emergence of a complicated structure with two centers in the inner region of the TC (Fig. 6d). During hours 11–18, the two centers underwent cyclonic rotation (Figs. 6e–h). Coincident with the occurrence of the complicated structure with two centers, an abrupt change in direction of the motion of the TC occurs from west-northwestward to west-southwestward (Fig. 5). Notice that the EV has no any significant changes for hours 11–14 (Figs. 6d–g), we believe that the interaction between the mesoscale vortex $a$and the TC may have been a prime contributor to the change of the TC track.

3.4.2 *Indirect influence*

Figure 7 derived from the three simulations in EXA_1, EXB_3, and EXB_4 indicates that the TC has a faster and eventually more westward propagation in EXB_3 than in EXB_4. The evolution sequence of vorticity distribution in EXB_3 is located in Fig. 8. Two mesoscale vortices lie to the northeast of the EV center at t= 0 h (Fig. 8a). They move anticlockwise and merge together during hours 0–6 (Figs. 8b, c). Afterward, the merged vortex shifted into the inner region of the EV, bringing about the latter intensification (Figs. 8d–h).

In the initial field of EXB_4, a mesoscale vortex was located to the south of the EV center (Fig. 9a). However, it did not move into the inner region of the EV in the whole integration process (Figs. 9b–h), meaning that the scale interaction had no significant role in changing the intensity of the EV. Figure 10 shows the evolutions in time of the intensity I_E of the EV in EXA_1, B_3, and B_4, respectively, where I_E is defined as the vorticity at the EV center. The intensity was approximately conserved in EXA_1 (curve A) and EXB_4 (curve V). Whereas it increasesd after t=12 h significantly in EXB_3 (curve T).

A more intense EV may be expected to produce a more strong steering flow. A TC steering flow was defined as radial-band averages of the wind at various distances from the TC center (Chan and Gray, 1982). The range of the radial band may have various values for various TCs. In this work, R_m is defined as the radius of maximum wind speed of the TC in the three simulations; because R_m changes in the interval of 100 km $\leqslant R_m \leqslant$130 km in the whole integration, the wind averaged in the region of 100 km$\leqslant r \leqslant$200 km, as well as the wind averaged in the region of 130 km$\leqslant r \leqslant$260 km were calculated. The mean value of the two winds is defined as the steering current V_E of the TC. Results show that V_E=1.25 m s^{-1}, 1.43 m s^{-1}, and 1.28 m s^{-1} in EXA_1, EXB_3, and EXB_4, respectively, demonstrating that the steering flow is the strongest in EXB_3 and that they are similar in EXA_1 and EXB_4, which is consistent with the results in shown in Fig. 10.

4. Summary

As indicated by Elsberry (2007), the key point is

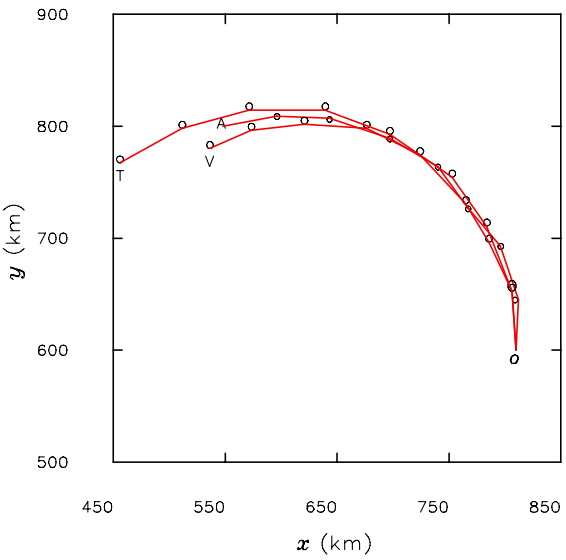

Fig. 7. Track of the center of the TC for EXA_1 (OA), for EXB_3 (OT), and for EXB_4 (OV). Circles denote TC center positions (3-h intervals).

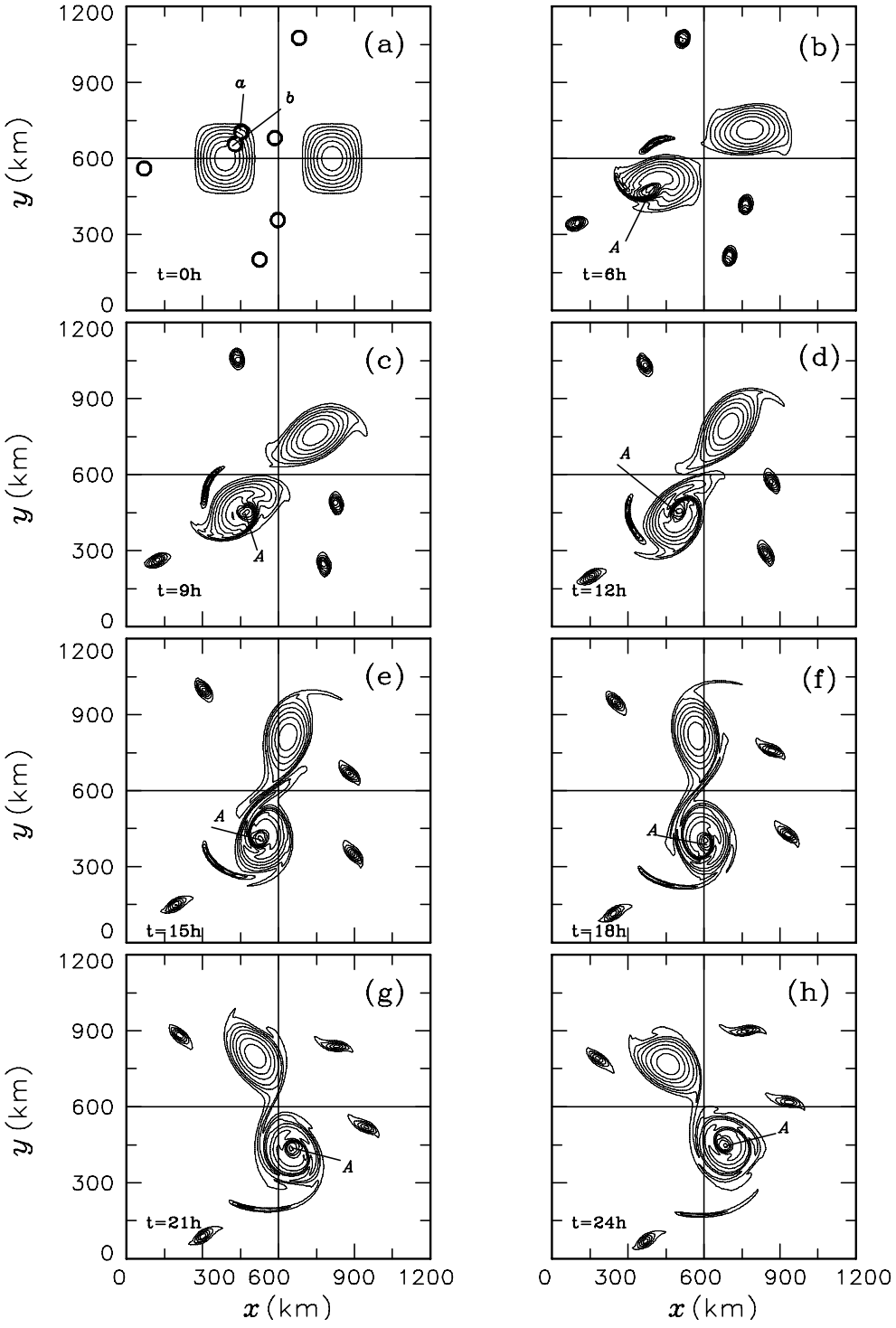

Fig. 8. Vorticity (contour interval 0.5×10^{-4} s^{-1}). At (a) t= 0, (b) 6 h, (c) 9 h, (d) 12 h, (e) 12 h, (f) 15 h, (g) 18 h, and (h) 24 h for EXB_3.

that TC motion is a multi-scale, nonlinear interaction problem. In this study, we explored the multi-scale nonlinear interaction and its effects on the TC track in a three component system, including an environment vortex (EV), a TC, and mesoscale vortices. In this study 62 simulations were performed with various initial mesoscale vorticity fields, which were generated stochastically by employing Reinaud's method. Our results show that the track deflections induced by the mesoscale vortices in 60% of the cases were smaller

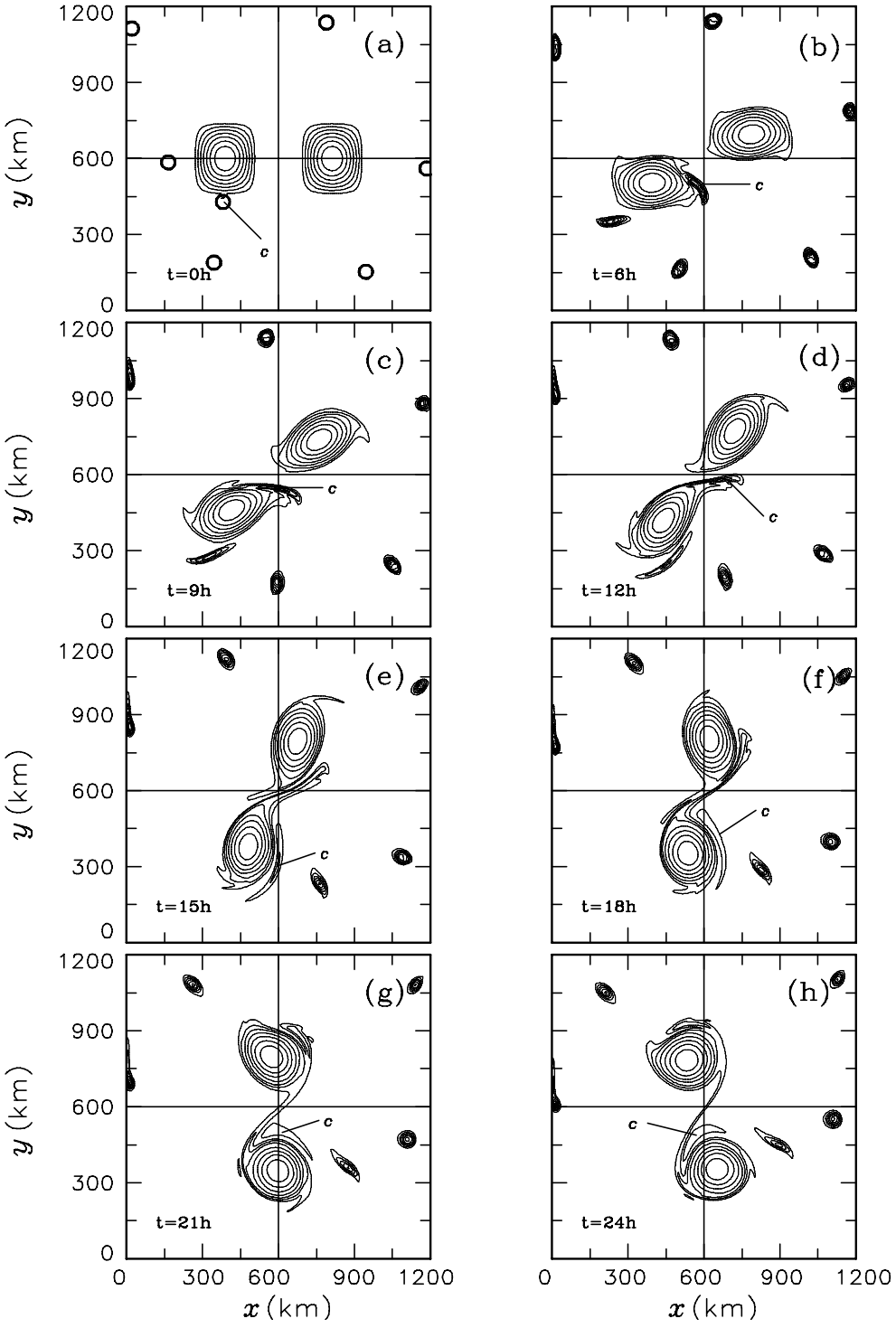

Fig. 9. As in Fig. 8, except for EXB_4.

than that deduced from the beta effect, while the track may have had a more significant deflection in the other cases.

In the multi-scale nonlinear interactions among the three components, two types can be highlighted: direct interaction and indirect influence. In the former, the adjacent mesoscale vortices directly modify the structure in the inner region of the TC. In the latter, they indirectly change the intensity of the EV. The both eventually produce different TC tracks.

The initial stochastic vorticity fields and the model used in this study were all idealized. A major limita-

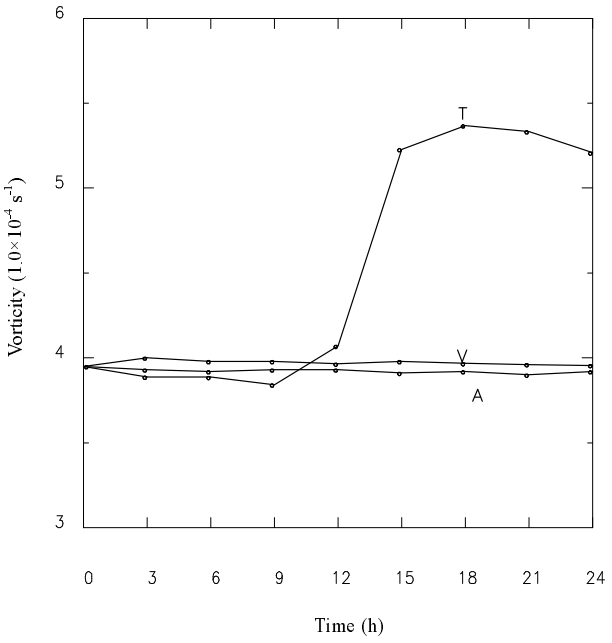

Fig. 10. Evolutions of vorticity at the center of the EV with time for EXA_1 (curve A), EXB_3 (curve T), and EXB_4 (curve V).

tion of this study was that very large-scale secondary circulations associated with convective heat, particularly from the TC, were not taken into account in these simulations. Understanding the sensitivity of the design of initial conditions such as the intensity of mesoscale vortices, and the distance between the vortices $\boldsymbol{W}$ and $\boldsymbol{E}$, as well as of computational parameters such as the area of the computation region remains limited. Further investigations that include these effects may be required to produce results that more closely reflect the circumstances in the real atmosphere.

Acknowledgements. This work was supported by the National Natural Science Foundation of China (Grant Nos. 40775038, 40875031 and 40975036).

REFERENCES

Asselin, R., 1972: Frequency filter for time integrations. *Mon. Wea. Rev.*, **109**, 18–36.

Basdevant, C., B. Legras, R. Sadourny, and M. Beland, 1981: A study of barotropic model flows: Intermittency, waves and predictability. *J. Atmos. Sci.*, **38**, 2305–2326.

Chan, J. C. L., and W. M. Gray, 1982: Tropical cyclone movement and surrounding flow relationships. *Mon. Wea. Rev.*, **110**, 1354–1374.

Chan, J. C. L., and R. T. Williams, 1987: Analytical and numerical studies of beta-effect in tropical cyclone motion. Part I: Zero mean flow. *J. Atmos. Sci.*, **44**, 1257–1264.

Chan, J. C. L., F. M. F. Ko, and Y. M. Lei, 2002: Relationship between potential vorticity tendency and tropical cyclone motion. *J. Atmos. Sci.*, **59**, 1317–1336.

Chen, L., and Z. Luo, 2006: The effect of interaction between mesoscale system and typhoon on its motion and structure change. Preprints, *27th Conf. on Hurricanes and Tropical Meteorology,* Monterey, CA., Amer. Meteor. Soc., 8B1. [Available online at http://ams.confex.com/ams/27 Hurricanes]

DeMaria, M., 1985: Tropical cyclone motion in a nondivergent barotropic model. *Mon. Wea. Rev.*, **113**, 1199–1210.

Dong, K., and C. J. Neumann, 1986: The relationship between tropical cyclone motion and environmental geostrophic flows. *Mon. Wea. Rev.*, **114**, 115–122.

Elsberry, R. L., Ed., 1995: Global perspectives of tropical cyclones. World Meteorological Organization WMO-/TD-NO. 693, Rep. TCP-38, 289pp.

Elsberry, R. L., 2007: Recent advances in tropical cyclone track forecasting techniques that impact disaster prevention and mitigation. *International Training Workshop on Tropical Cyclone Disaster Reduction,* WMO, CASWGTM, Guangzhou, China, 1–7.

Enagonio, J., and M. T. Montgomery, 2001: Tropical cyclogenesis via convectively forced vortex Rossby waves in a shallow-water primitive equation model. *J. Atmos. Sci.*, **58**, 685–705.

Feynman, R. P., 1961: There's plenty of room at the bottom. *Miniaturization*, Gilbert, Ed., Reinhold, New York, 282–289.

Fiorino, M., and R. L. Elsberry, 1989: Some aspects of vortex structure in tropical cyclone motion. *J. Atmos, Sci.*, **46**, 975–990.

Gentry, R. C., T. T. Fujita, and R. C. Sheets, 1968: Aircraft, spacecraft, satellite and radar observations of Hurricane Gladys. *J. Appl. Meteor*, **9**, 837–850.

Ishioka, K., J. Hasegawa, and S. Yoden, 2006: Asymmetrization mechanism of jet profiles in decaying β-plane turbulence. *J. Atmos. Sci.*, **64**, 3354–3361.

Luo, Z., and C. Liu, 2006: Diversity of microenvironments and the complexity of vortex motion. *Geophys. Res. Lett.*, **33**, L24805, doi: 10.1029/2006GL027765.

Reinaud, J. N., D. G. Dritschel, and C. R. Koudella, 2003: The shape of vortices in quasi-geostrophic turbulence. *J. Fluid Mech.*, **474**, 175–192.

Tian, Y., and Z. Luo, 1994: Vertical structure of beta gyres and its effect on tropical cyclone motion. *Adv. Atmos. Sci.*, **11**, 43–50.

Velden, C. S., and L. M. Leslie, 1991: The basic relationship between tropical cyclone intensity and the depth of the environmental steering layer in the Australian region. *Weather and Forecasting*, **6**, 244–253.

Wang, D., X. Liang, and Y. Duan, 2006: Impact of four-dimensional variational data assimilation of atmospheric motion vectors on tropical cyclone track forecasts. *Wea. Forecasting*, **21**, 663–669.

Willoughby, H. E., 1992: Linear motion of a shallow-water barotropic vortex as an initial value problem. *J. Atmos. Sci.*, **49**, 2015–2031.

Wu, C.–C., and Y. Kurihara, 1996: A numerical study of the feedback mechanisms of hurricane-environment interaction on hurricane movement from a potential vorticity perspective. *J. Atmos. Sci.*, **53**, 2264–2282.

Wu, C.–C., J.–H. Chen, P.–H. Lin, and K.–H. Chou, 2006: Targeted observations of tropical cyclone movement based on the adjoint-derived sensitivity steering vector. *27th Conf. on Hurricanes and Tropical Meteorology,* Monterey, CA., Amer. Meteor. Soc., 8B2. [Available online from http://ams.confex. com/ams/27 Hurricanes]

Wu, L.-G., and B. Wang, 2000: A potential vorticity tendency diagnostic approach for tropical cyclone motion. *Mon. Wea. Rev.*, **128**, 1899–1911.

Yu, H., W. Huang, Y. Duan, J. C. L. Chan, and R. Yu, 2006: A simulation study on pre-landfall erratic track of Typhoon Haitang (2005) with GRAPES TCM. Preprints, *27th Conf. on Hurricanes and Tropical Meteorology,* Monterey, CA., Amer. Meteor. Soc., 8B6. [Available online from http://ams.confex.com/ams/27Hurricanes]